Combustion, Explosion, and Shock Waves, Vol. 34, No. 2, 1998

Mathematical Study of Thermal Explosion of a Magnesium Particle with Allowance for Metal Evaporation

Yu. A. Gosteev[1] and A. V. Fedorov[1]

UDC 534.222.2; 662.612.32

Translated from *Fizika Goreniya i Vzryva*, Vol. 34, No. 2, pp. 39–46, March–April, 1998.
Original article submitted January 20, 1997.

A catastrophe/ignition manifold for a model of thermal explosion of a magnesium particle is constructed. The model takes into account the chemical oxidation reaction, metal evaporation, and convective heat exchange with the ambient gas. This made it possible to determine the types of heat dynamics of the particle in the plane of bifurcation parameters of the model (to locate ignition, extinction, and regular-heating regions), to find the kinetic constants in the empirical law of ignition on the basis of experimental data, and to show the stability of the integral parameter of the ignition delay in relation to sets of kinetic constants determined for mathematical models with and without account for metal evaporation.

Papers dealing with physicomathematical simulation of ignition of small magnesium particles were reviewed by Fedorov and Gosteev in [1–3]. In addition, they studied this phenomenon by methods of elementary catastrophe theory and numerically within the framework of pointwise and distributed models that take into account a heterogeneous chemical reaction. At the same time, the literature data indicate that it is important to take into account evaporation of the metal and its oxide from the particle surface. This phenomenon was ignored in [1–3]. It is also of interest to study this process from the viewpoint of the general theory of thermal explosion of systems with two chemical reactions having different characteristic times and activation energies [4]. In the present paper, we construct a catastrophe/ignition manifold for a model of thermal explosion of a magnesium particle that takes into account metal evaporation and also determine the types of particle thermodynamics in the plane of bifurcation parameters of the model. Calculation data obtained using different models are compared.

1. GOVERNING EQUATION OF THE MATHEMATICAL MODEL

We study the effect of metal evaporation on particle ignition under the action of a high-temperature ambient gas (see, for example, [5]) within the framework of the pointwise model [6]. A similar mathematical model appears in studying the features of the transformation in a system with two parallel chemical reactions, one of which is exothermic and the other is endothermic [4].

The equation that describes the evolution of the particle temperature in time has the form [6]

$$\frac{1}{3}\frac{c_s r_s}{qk}\frac{dT}{dt} = \exp\left(-\frac{E}{RT}\right) - c\exp\left(-\frac{E_1}{RT}\right) - \tilde{\alpha}(T-\tilde{T}) \equiv g(T), \quad (1)$$

where $\tilde{\alpha} = \lambda \mathrm{Nu}/2qr_s\rho_s k$, $k = k_0 c_{\mathrm{ox}}$, $c = v/k$; c_s and ρ_s are the heat capacity and density of the metal, respectively, and r_s is the particle radius; c_{ox} is the mass concentration of the oxidizer; Nu is the Nusselt number; q, E, and k_0 are the thermal effect, activation energy, and preexponent of the oxidation reaction; E_1 is the heat of evaporation; λ and $\tilde{T}$ are the thermal conductivity and temperature of the ambient medium.

To analyze qualitatively the solution of the Cauchy problem for (1)

$$t = 0: \quad T = T_0, \quad (1a)$$

we consider the zero isocline of Eq. (1) in the domain of the variables T, $\tilde{\alpha}$, $\tilde{T}$, c, E, and E_1 using methods of elementary catastrophe theory.

[1] Institute of Theoretical and Applied Mechanics, Siberian Division, Russian Academy of Sciences, Novosibirsk 630090.

0010-5082/98/3402-0151 $20.00

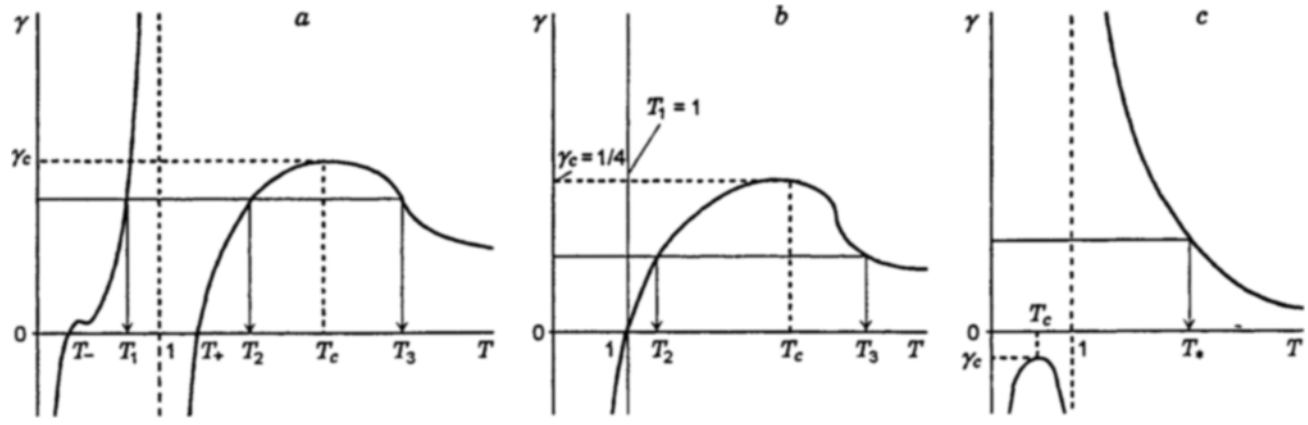

Fig. 1. Diagram of the roots for determination of TCP: $\tilde{T} < 1/2$ (a), $\tilde{T} = 1/2$ (b), and $\tilde{T} > 1/2$ (c).

2. STUDY OF THE IGNITION MANIFOLD

2.1. Basic Relationships for Construction of a Catastrophe/Ignition Manifold. Similarly to [1, 2, 7], we consider conditions that allow us to find triply degenerate critical points (TCP) of the potential function $G(T) = \int g(T)\,dT$:

$$e^{-2/T} - ce^{-2/\gamma T} = \alpha(T - \tilde{T}),$$
$$\frac{2}{T^2}e^{-2/T} - \frac{2}{T^2}\frac{c}{\gamma}e^{-2/\gamma T} = \alpha, \qquad (2)$$
$$e^{-2/T}\left(\frac{1}{T} - 1\right) - \frac{c}{\gamma}e^{-2/\gamma T}\left(\frac{1}{\gamma T} - 1\right) = 0.$$

The quantity $T_s = E/2R$ is taken as a temperature scale, and the parameters $\gamma = E/E_1$ and $\alpha = \bar{\alpha}T_s$ are introduced. The solution of system (2), which determines the TCP (T_*, α_*, c_*) in the space (T, α, c), reduces to the solution of the equation

$$\gamma T^2(T-1) = T^2 - 2T + 2\tilde{T}$$

or (3)

$$P(T) \equiv \gamma T^3 - (\gamma+1)T^2 + 2T - 2\tilde{T} = 0.$$

It follows from (3) that the roots of this equation depend parametrically on γ and $\tilde{T}$. For $\tilde{T} < 0.5$, the following representation is valid:

$$\gamma = \frac{(T - T_+)(T - T_-)}{T^2(T-1)}, \qquad (4)$$

where $T_\pm = 1 \pm \sqrt{1 - 2\tilde{T}}$.

We analyze qualitatively the solutions of Eq. (3) using a diagram of the roots $T_* = T_*(\gamma, \tilde{T})$ (Fig. 1). The results of this analysis can be formulated as follows.

• Statement 1 (*on the existence of triply degenerate critical points*). The number and sequence of the roots of Eq. (3) are determined, depending on γ and $\tilde{T}$, as follows.

(1) Let $\tilde{T} < 1/2$. Then

(a) if $0 < \gamma \leqslant \gamma_c$, there are three real roots $T_* = T_{1,2,3}$ $(T_- < T_1 < 1 < T_2 < T_c < T_3)$;

(b) if $\gamma > \gamma_c$, there are one real root T_* $(T_- < T_* < 1)$ and two complex-conjugate roots.

(2) Let $\tilde{T} = 1/2$. Then

(a) if $0 < \gamma \leqslant \gamma_c = 1/4$, there are three real roots $T_* = T_{1,2,3}$ $(T_1 = 1 < T_2 < T_c < T_3)$, and $T_2 = T_3$ if $\gamma = \gamma_c$;

(b) if $\gamma > \gamma_c$, there are one real root $T_* = 1$ and two complex-conjugate roots.

(3) Let $\tilde{T} > 1/2$. Then there is one real root $T_* > 1$ for all $\gamma > 0$.

Here the critical quantity is

$$\gamma_c = \max\gamma(T)\big|_{T>1} = \gamma_c(\tilde{T}) \text{ for } \tilde{T} \leqslant 1/2.$$

The function $\gamma_c(\tilde{T})$ is defined parametrically: $\gamma_c = \gamma(T_c)$ according to (4), and the relationship $\tilde{T} = H(T_c)$ follows from the equality $\left.\frac{d\gamma(T)}{dT}\right|_{T=T_c} = 0$. The dependence $\gamma_c(\tilde{T})$ is plotted in Fig. 2. It is seen that, for real values of $\tilde{T}$ ($\leqslant 0.2$–0.3), the value of γ_c is always smaller than unity. The proof of Statement 1 follows from elementary constructions of the function $\gamma(T)$ defined according (4) and its continuity for $T > 1$.

2.2. Asymptotic and Numerical Representation of the Roots for TCP. We write asymptotic expressions for the real solutions of Eq. (3) under the conditions $\gamma \ll 1$ and $\gamma \gg 1$.

• Statement 2 [*on the asymptotic representation of the roots of Eq.* (3)]. Let $\tilde{T} \leqslant 1/2$. Then Eq. (3)

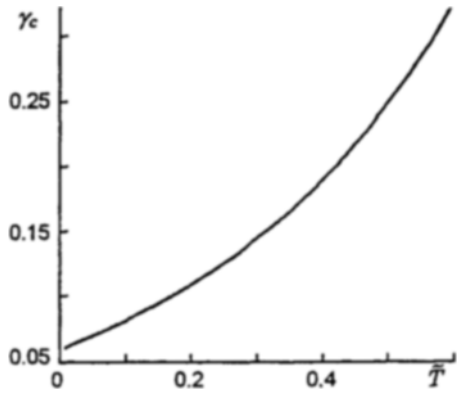

Fig. 2. Critical quantity γ_c versus the ambient temperature.

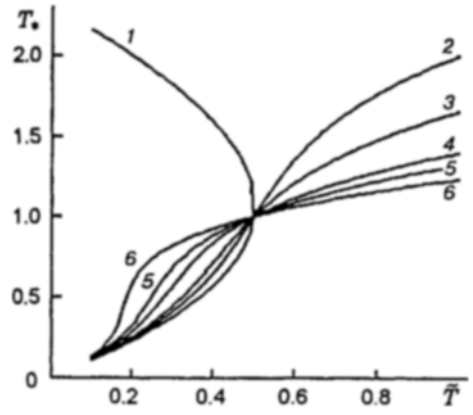

Fig. 3. Diagram of the roots $T_* = T_*(\tilde{T}, \gamma)$ for determination of TCP: $\gamma = 0.1$ (1), 0.5 (2), 0.8 (3), 1.5 (4), 2.0 (5), and 3.0 (6) (for the case $\gamma = 0.1$, the branch of the third, largest root is not shown).

has three real approximate solutions for $\gamma \ll 1$:

$$T_{1,2} = T_{\mp} + \gamma \frac{T_{\mp}^2}{2} + \gamma^2 \frac{T_{\mp}^3}{2}\left(1 - \frac{3}{2}T_{\mp}\right) + O(\gamma^3),$$

$$T_3 = \frac{\gamma + 1}{\gamma} - (T_1 + T_2) + O(\gamma^3),$$

and a unique real approximate solution for $\gamma \gg 1$:

$$T_* = 1 + \gamma^{-1}(2\tilde{T} - 1) - \gamma^{-2}2(2\tilde{T} - 1)^2 + O(\gamma^{-3}).$$

The accuracy of the above expansions can be evaluated using the numerical data presented in Tables 1 and 2.

In the general case, where γ is finite, Eq. (3) was solved numerically. The results are given in Fig. 3 as a diagram of the roots $T_* = T_*(\tilde{T}, \gamma)$ for a number of values of γ.

TABLE 1

Accuracy of the Asymptotic Solutions of Eq. (3) for $\gamma \ll 1$ ($\tilde{T} = 0.1$)

Root and residual	$\gamma = 0.001$	$\gamma = 0.01$	$\gamma = 0.1$
T_1	0.10561	0.10563	0.10613
$P(T_1)$	$-2 \cdot 10^{-8}$	$2 \cdot 10^{-8}$	$-1.51 \cdot 10^{-6}$
T_2	1.8962	1.9117	2.0112
$P(T_2)$	$2 \cdot 10^{-5}$	$2 \cdot 10^{-4}$	$1.86 \cdot 10^{-1}$
T_3	998.9982	98.9982	8.88266
$P(T_3)$	$3.64 \cdot 10^{-2}$	1.6072	−0.9

TABLE 2

Accuracy of the Asymptotic Solutions of Eq. (3) for $\gamma \gg 1$ ($\tilde{T} = 0.1$)

Root and residual	$\gamma = 2$	$\gamma = 10$	$\gamma = 100$
T_*	0.9200	0.9320	0.9920
$P(T_*)$	−0.39	$2 \cdot 10^{-2}$	$1.1 \cdot 10^{-3}$

We note that, in the case important in practice where $\gamma > \gamma_c < 1$, the catastrophe manifold has a single triply degenerate critical point, as in the ignition model without evaporation. A new circumstance is the existence of a catastrophe manifold with three TCP when evaporation is much more intense than oxidation ($E \ll E_1$). This indicates the presence of a complicated heat dynamics in the system with this relationship of parameters and the possibility of nontrivial scenarios of particle ignition.

We also present a bifurcation diagram for the roots of Eq. (3) in the plane $(\gamma, \tilde{T})$, which separates the domains of parameters with a different number of TCP. It is obtained by plotting the curves $\tilde{T} = \tilde{T}_{1,2}(\gamma)$ along which the discriminant of this cubic

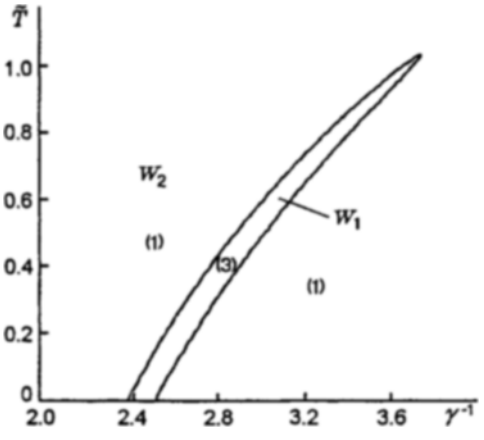

Fig. 4. Partition of the plane of parameters $(\gamma, \tilde{T})$ into domains with one (W_2) and three (W_1) TCP (the figures in the parentheses refer to the number of TCP).

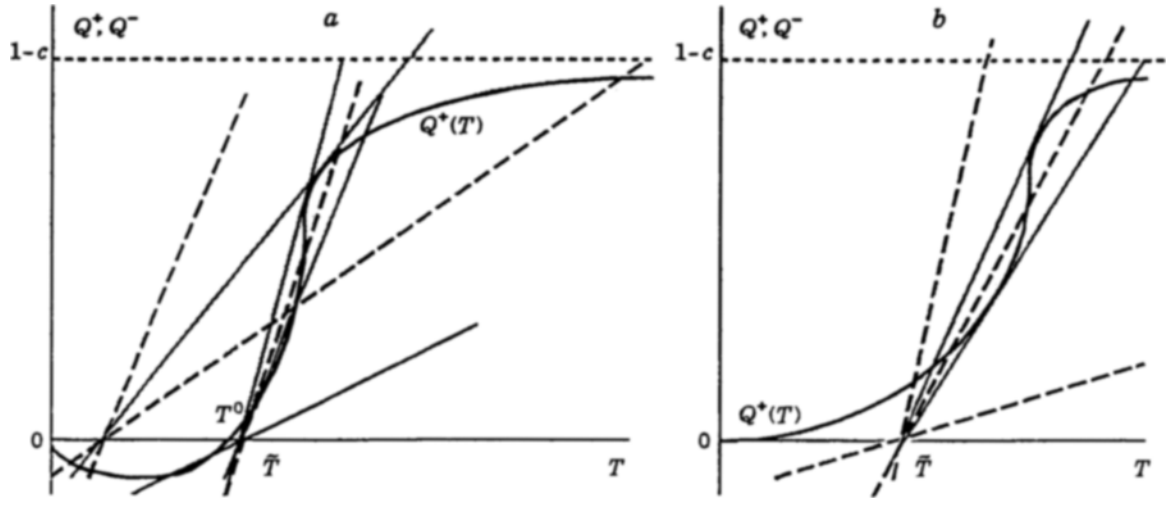

Fig. 5. Semenov's diagram, depending on the stationary adiabatic temperature T_0 (for $c < 1$): $T_0 > 0$ (a) and $T_0 < 0$ (b); the dashed curves show various positions of the convective heat output curve $Q^-(T)$, and the solid straight lines show the extreme (tangent) positions of this curve.

equation vanishes (Fig. 4).

3. BIFURCATION DIAGRAM AND DETERMINATION OF THE KINETIC CONSTANTS

3.1. Construction of Zero Isoclines of Eq. (1) in Cross Sections c = const of the Equilibrium Surface. We turn to Fig. 5, which shows Semenov's diagram with curves of the total heat input

$$Q^+(T) = e^{-2/T} - ce^{-2/\gamma T}$$

and the heat output

$$Q^-(T) = \alpha(T - \tilde{T}).$$

The equation $Q^+(T) = 0$ has the roots

$$T = 0 \quad \text{and} \quad T = T^0 = \frac{2(\gamma - 1)}{\gamma \ln(1/c)},$$

where T^0 has the meaning of the stationary adiabatic temperature in the system.

Obviously, various cases of tangency of the curves $Q^+(T)$ and $Q^-(T)$ are possible, depending on the sign of T^0 and the relationship between $\tilde{T}$ and T^0 (we confine ourselves to the variant $c < 1$). The results of this analysis can be summarized as follows.

• Statement 3 (*on the critical conditions of a thermal explosion*).

(1) Let $T^0 > 0$. Then

(1.1) if $\tilde{T} < T^0$, there is one tangent point (T_t, α_t), and

— for $\alpha < \alpha_t$, there are three equilibrium positions located at $(0, \tilde{T})$, (T^0, T_t), and (T_t, ∞), respectively;

— for $\alpha > \alpha_t$, there is one equilibrium position located at $(0, \tilde{T})$;

(1.2) if $\tilde{T} > T^0$, there are three tangent points $(T_{t,i}, \alpha_{t,i})_{i=1,2,3}$, numbered in increasing order of α_t, and

— for $\alpha < \alpha_{t,1}$, there are three equilibrium positions located at $(0, T_{t,1})$, $(T_{t,1}, T^0)$, and $(T_{t,3}, \infty)$, respectively;

— for $\alpha_{t,1} < \alpha < \alpha_{t,2}$, there is one equilibrium position located at $(T_{t,3}, \infty)$;

— for $\alpha_{t,2} < \alpha < \alpha_{t,3}$, there are three equilibrium positions located at $(\tilde{T}, T_{t,2})$, $(T_{t,2}, T_{t,3})$, and $(T_{t,3}, \infty)$, respectively;

— for $\alpha > \alpha_{t,3}$, there is one equilibrium position located at $(\tilde{T}, T_{t,2})$.

(2) If $T^0 < 0$, there are two tangent points $(T_{t,i}, \alpha_{t,i})_{i=1,2}$, and

— for $\alpha < \alpha_{t,1}$, there is one equilibrium position located at $(T_{t,2}, \infty)$;

— for $\alpha_{t,1} < \alpha < \alpha_{t,2}$, there are three equilibrium positions located at $(\tilde{T}, T_{t,1})$, $(T_{t,1}, T_{t,2})$, and $(T_{t,2}, \infty)$, respectively;

— for $\alpha > \alpha_{t,2}$, there is one equilibrium position located at $(\tilde{T}, T_{t,1})$.

The foregoing Statement 3 can easily be proved by a qualitative analysis of the curves $Q^{\pm}(T)$ (Fig. 5).

We formulate some properties of the source function $Q^+(T)$ that are needed to construct the equilibrium surface:

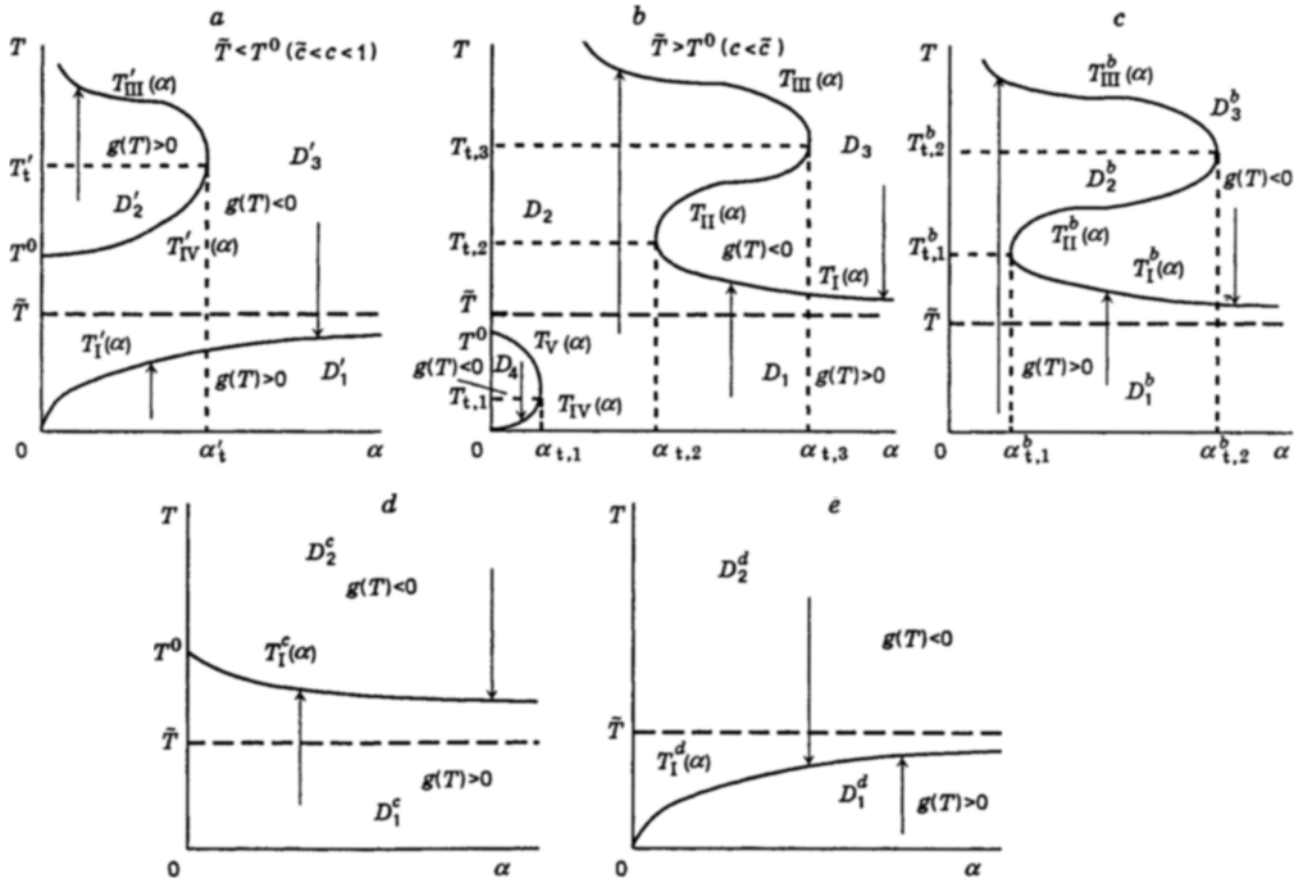

Fig. 6. Construction of the ignition manifold (typical cross sections $c = \text{const}$): a, b) $0 < c < 1$ and $\gamma > 1$; c) $0 < c < 1$ and $\gamma < 1$; d) $c > 1$ and $\gamma < 1$; e) $c > 1$ and $\gamma > 1$; the arrows indicate possible variants of particle heating/cooling.

(1) $Q^+(T) \to 0$ for $T \to 0$;

(2) $Q^+(T) \to (1-c)$ for $T \to \infty$;

(3) $T^0 > 0$ if

(a) $0 < c < 1$ and $\gamma > 1$, or

(b) $c > 1$ and $\gamma < 1$;

$T^0 < 0$ if

(c) $0 < c < 1$ and $\gamma < 1$ or

(d) $c > 1$ and $\gamma > 1$.

We analyze typical cross sections $c = \text{const}$ of the catastrophe manifold, which is necessary to describe the dynamics of the particle temperature.

3.2. Bifurcation Diagram. Types of Heat Dynamics. After determining the TCP coordinates, we can build images of the curved folds on the plane (α, c). They are the projections of the corresponding doubly degenerate critical points onto the equilibrium surface (catastrophe manifold) in the space (T, α, c) that is defined by the first equation in (2). In parametric form, the fold lines are determined from the relations

$$c = \gamma \frac{T^2 - 2(T-\tilde{T})}{\gamma T^2 - 2(T-\tilde{T})} e^{-2(\gamma-1)/\gamma T}$$
$$\alpha = \frac{2(\gamma-1)}{\gamma T^2 - 2(T-\tilde{T})} e^{-2/T}, \tag{5}$$

where the parameter T runs along the positive semiaxis $0 \leqslant T < \infty$. The fold lines (5) have singularities determined by the roots of the denominators. We find these roots: $T_{v\pm} = (1/\gamma)(1 \pm \sqrt{1-2\gamma\tilde{T}})$. The function $c(T)$ vanishes at the points $T = T_\pm$. Thus, the form of the fold lines (5) depends significantly on the mutual position of the roots $T_{v\pm}$ and $T_\pm$. In particular, we have $\gamma T_{v-} < T_- < T_+ < T_{v+}$ for $\gamma < 1$ and $T_- < \gamma T_{v-} < T_{v+} < T_+$ for $\gamma > 1$.

Based on the properties of the function $Q^+(T)$ and the evaluations of $T_{v\pm}$, we can construct a qualitative shape of the catastrophe manifold in cross sections $c = \text{const}$ (Fig. 6). Typical regions are determined below.

We first consider a situation where the oxidation reaction is more intense than evaporation, which corresponds to $\gamma > 1$. As shown in Fig. 6b, if $T^0 \leqslant \tilde{T}$, particle heating can occur in two ways, depending on the values of the convective heat-transfer coefficient α and the temperature $\tilde{T}$:

— regular heating to a temperature higher than $\tilde{T}$ for $\alpha > \alpha_{t,2}$ and $T_0 < T_{\mathrm{I}}(\alpha)$ or a temperature not greater than $\tilde{T}$ for $\alpha < \alpha_{t,1}$ and $T_0 < T_{\mathrm{IV}}(\alpha)$;

— ignition for $\alpha_{t,1} < \alpha < \alpha_{t,2}$ and $T_0 < T_{\mathrm{III}}(\alpha)$, or for $\alpha < \alpha_{t,1}$ and $T_0 > T_{\mathrm{V}}(\alpha)$, or for $\alpha_{t,2} < \alpha < \alpha_{t,3}$ and $T_{\mathrm{II}}(\alpha) < T_0 < T_{\mathrm{III}}(\alpha)$.

Of particular interest is the presence of a bilateral limit of ignition with respect to the convective heat-transfer coefficient ($\alpha_{t,1}$ and $\alpha_{t,2}$), which can be associated with the "provoking" role of convective heat transfer from the gas in the range of particle temperatures $0 < T < \tilde{T}$. The appearance of an additional domain D_4 of low-temperature extinction is noteworthy.

According to Fig. 6a, for $T^0 > \tilde{T}$ particle heating is limited from above by the temperature $T'_{\mathrm{I}}(\alpha) > \tilde{T}$ if its initial temperature does not exceed $T'_{\mathrm{I}}(\alpha)$, otherwise particle extinction or ignition can occur depending on whether the point (α, T_0) belongs to the domain D'_3 or D'_2, respectively.

Finally, at $v > k$ (for $\gamma > 1$), heat production is always compensated by heat removal at a particle temperature that does not exceed the ambient temperature, and a thermal explosion cannot occur (see Fig. 6e). The contribution of evaporation to the total heat loss is quite substantial.

We now consider the case where the heat of evaporation is greater than the activation energy for oxidation ($\gamma_c < \gamma < 1$). The thermal evolution of a particle (for $v < k$) (see Fig. 6c) is completely similar to the behavior predicted by a model that ignores evaporation:

— regular particle heating if the convective heat transfer coefficient is larger than the critical value $\alpha^b_{t,1}$ and the initial temperature is lower than $T^b_{\mathrm{I}}(\alpha)$;

— ignition if $\alpha < \alpha^b_{t,1}$ and $T_0 < T^b_{\mathrm{III}}(b)$ or $\alpha^b_{t,1} < \alpha < \alpha^b_{t,2}$ and $T^b_{\mathrm{II}}(\alpha) < T_0 < T^b_{\mathrm{III}}(\alpha)$;

— particle extinction if the parameters (α, T_0) belong to the region D^b_3.

In the case $v > k$ (see Fig. 6d), the fraction of vaporization in the heat loss is comparatively small, and regular explosionless heating of a particle to a temperature higher than the ambient temperature but lower than its equilibrium adiabatic temperature always occurs.

Using the analysis of zero isoclines in cross sections $c = \mathrm{const}$, we can classify in detail the types of heat dynamics of a particle. Before formulation of a statement, we determine typical regions of the parametric plane (α, T):

$$D_1 = \{(\alpha, T) : \alpha \in (\alpha_{t,2}, \infty), T \in (0, T_{\mathrm{I}}(\alpha))\},$$

$$D_2 = \{(\alpha, T) : \alpha \in (0, \alpha_{t,1}), T \in (0, T_{\mathrm{IV}}(\alpha))\}$$
$$\cup\{(\alpha, T) : \alpha \in (0, \alpha_{t,1}), T \in (T_{\mathrm{V}}(\alpha), T_{\mathrm{III}}(\alpha))\}$$
$$\cup\{(\alpha, T) : \alpha \in (\alpha_{t,1}, \alpha_{t,2}), T \in (0, T_{\mathrm{III}}(\alpha))\}$$
$$\cup\{(\alpha, T) : \alpha \in (\alpha_{t,2}, \alpha_{t,3}), T \in (T_{\mathrm{II}}(\alpha), T_{\mathrm{III}}(\alpha))\},$$

$$D_4 = \{(\alpha, T) : \alpha \in (0, \alpha_{t,1}), T \in (T_{\mathrm{IV}}(\alpha), T_{\mathrm{V}}(\alpha))\},$$

the domain D_3 is $\{(\alpha, T)\}\backslash(D_1 \cup D_2 \cup D_3)$ (see Fig. 6b);

$$D'_1 = \{(\alpha, T) : \alpha \in (0, \infty), T \in (0, T'_{\mathrm{I}}(\alpha))\},$$

$$D'_2 = \{(\alpha, T) : \alpha \in (0, \alpha'_{\mathrm{t}}), T \in (T'_{\mathrm{IV}}(\alpha), T'_{\mathrm{III}}(\alpha))\},$$

the domain D'_3 is $\{(\alpha, T)\}\backslash(D'_1 \cup D'_2)$ (see Fig. 6a);

$$D^b_1 = \{(\alpha, T) : \alpha \in (\alpha^b_{t,1}, \infty), T \in (0, T^b_{\mathrm{I}}(\alpha))\},$$

$$D^b_2 = \{(\alpha, T) : \alpha \in (0, \alpha^b_{t,1}), T \in (0, T^b_{\mathrm{III}}(\alpha))\}$$
$$\cup\{(\alpha, T) :\in (\alpha^b_{t,1}, \alpha^b_{t,2}), T \in (T^b_{\mathrm{II}}(\alpha), T^b_{\mathrm{III}}(\alpha))\},$$

the domain D^b_3 is $\{(\alpha, T)\}\backslash(D^b_1 \cup D^b_2)$ (see Fig. 6c);

$$D^c_1 = \{(\alpha, T) : \alpha \in (0, \infty), T \in (0, T^c_{\mathrm{I}}(\alpha))\},$$

the domain D^c_2 is $\{(\alpha, T)\}\backslash D^c_1$ (see Fig. 6d);

$$D^d_1 = \{(\alpha, T) : \alpha \in (0, \infty), T \in (0, T^d_{\mathrm{I}}(\alpha))\},$$

the domain D^d_2 is $\{(\alpha, T)\}\backslash D^d_1$.

Now the following statement is valid.

• Statement 4 (*types of heat dynamics of the particle temperature*).

(1) If $\gamma > 1$ and

(1.1) $c < \tilde{c}$, then

— for $(\alpha, T_0) \in D_1$, the temperature stabilizes on the lower branch $T_{\mathrm{I}}(\alpha) > \tilde{T}$; for $(\alpha, T_0) \in D_2$, the solution describes ignition and stabilizes on the upper branch $T_{\mathrm{III}}(\alpha)$ of steady states;

— for $(\alpha, T_0) \in D_3$, the solution describes particle extinction, i.e., the temperature stabilizes on the branch $T_I(\alpha)$ for $\alpha > \alpha_{t,3}$ [or $\alpha \in (\alpha_{t,2}, \alpha_{t,3})$] and $T_0 \in (T_{\mathrm{I}}(\alpha), T_{\mathrm{II}}(\alpha))$, and on the branch $T_{\mathrm{III}}(\alpha)$ for $\alpha < \alpha_{t,3}$ and $T_0 > T_{\mathrm{III}}(\alpha)$;

— for $(\alpha, T_0) \in D_4$, the solution describes particle extinction, and the temperature stabilizes on the branch $T_{\mathrm{IV}}(\alpha)$;

(1.2) $\tilde{c} < c < 1$, then

— for $(\alpha, T_0) \in D'_1$, the solution describes explosionless heating with transition to equilibrium on the lower branch $T'_{\mathrm{I}}(\alpha) < \tilde{T}$;

— for $(\alpha, T_0) \in D'_2$, the ignition regime with temperature stabilization on the upper stable branch $T'_{\mathrm{III}}(\alpha)$ of steady states occurs;

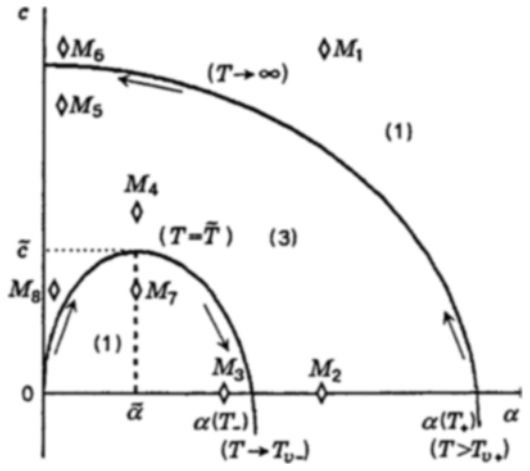

Fig. 7. Bifurcation diagram of the system in the plane (α, c) (for $\gamma = 1.4$ and $\tilde{T} = 0.18$): points $\diamond$ refer to the control points M_j, the figures in the parentheses denote the number of TCP.

— for $(\alpha, T_0) \in D_3'$, the solution describes particle extinction with temperature stabilization on the branch $T_{\mathrm{I}}'(\alpha)$ for $\alpha > \alpha_t'$ [or $\alpha \in (0, \alpha_t')$] and $T_0 \in (T_{\mathrm{I}}'(\alpha), T_{\mathrm{IV}}'(\alpha))$, and on the branch $T_{\mathrm{III}}'(\alpha)$ for $\alpha \in (0, \alpha_t')$ and $T_0 > T_{\mathrm{III}}'(\alpha)$;

(1.3) $c > 1$, then

— for $(\alpha, T_0) \in D_1^d$, the solution describes explosionless heating of a particle with temperature stabilization on the lower branch $T_{\mathrm{I}}^d(\alpha) < \tilde{T}$;

— for $(\alpha, T_0) \in D_2^d$, the extinction regime with temperature stabilization on the branch $T_{\mathrm{I}}^d(\alpha)$ occurs.

(2) If $\gamma < 1$ and

(2.1) $0 < c < 1$, then

— for $(\alpha, T_0) \in D_1^b$, the solution describes explosionless heating with temperature stabilization on the lower steady-state branch $T_{\mathrm{I}}^b(\alpha) > \tilde{T}$;

— for $(\alpha, T_0) \in D_2^b$, the ignition regime with temperature stabilization on the upper branch $T_{\mathrm{III}}^b(\alpha)$ occurs;

— for $(\alpha, T_0) \in D_3^b$, particle extinction with temperature stabilization on the branch $T_I^b(\alpha)$ for $\alpha > \alpha_{t,2}^b$ [or $\alpha \in (\alpha_{t,1}^b, \alpha_{t,2}^b)$] and $T_0 \in (T_{\mathrm{I}}^b(\alpha), T_{\mathrm{II}}^b(b))$ and on the branch $T_{\mathrm{III}}^b(\alpha)$ for $\alpha < \alpha_{t,2}^b$ and $T_0 > T_{\mathrm{III}}^b(\alpha)$ occurs;

(2.2) $c > 1$, then

— for $(\alpha, T_0) \in D_1^c$, the solution describes explosionless heating with transition to equilibrium on the branch $T_{\mathrm{I}}^c(\alpha) > \tilde{T}$;

— for $(\alpha, T_0) \in D_2^c$, particle extinction occurs, and the temperature stabilizes on the branch $T_{\mathrm{I}}^c(\alpha)$.

Remark. We do not describe here the particle-temperature dynamics for the case where $\gamma < \gamma_c$ and the catastrophe manifold has three TCP.

3.3. Numerical Illustration of Statement 4. The following numerical example illustrates the construction of a catastrophe manifold in the case $\gamma > 1 > \gamma_c$, i.e., in the presence of a single TCP. The set of parameters $\gamma = 1.4$, $\tilde{T} = 0.18$, $T_+ = 1.8$, $T_- = 0.2$, $T_{v+} = 1.2173$, $T_{v-} = 0.2112$, $\tilde{c} = 4.18 \cdot 10^{-2}$, and $\tilde{\alpha} = 2.63 \cdot 10^{-4}$ corresponds to the TCP coordinate $T_* = 0.239$ and the bifurcation diagram in the plane (α, c) shown qualitatively in Fig. 7. The figures in the parentheses denote the number of thermal-equilibrium states in the system. The arrows indicate the direction in which the parameter T in Eqs. (5) increases along the fold lines. The points $\diamond$ marks the control points $M_j = (\alpha, c)_j$ $(j = 1, \ldots, 8)$ at which the Cauchy problem (1) and (1a) was solved. Geer's stiff-stable method was used to integrate (1) and (1a). The values of the parameters are listed in Table 3.

TABLE 3

Values of the Parameters at Control Points

Point number j	α_j	c_j	T^∞
1	0.1	1.1	0.1767
2	0.1	10^{-4}	0.1801
3	0.002	0	$4.98 \cdot 10^3$
4	$2.63 \cdot 10^{-4}$	0.1	0.1536
5	$1 \cdot 10^{-5}$	0.9	0.0562
6	$1 \cdot 10^{-5}$	1.1	0.0578
7	$2.63 \cdot 10^{-4}$	0.04	$3.65 \cdot 10^4$
8	$1 \cdot 10^{-5}$	0.04	0.110

Note. T^∞ is the final equilibrium temperature of the particle.

TABLE 4

Ignition Delay, msec

Radius, μm	Model of [1, 2]	Model under discussion
15	22.0	22.0
22	39.6	39.2
30	64.0	64.1
60	200.0	202.3
300	2200	1990
400	3800	3460
500	6000	5320
600	8500	7560

3.4. Determination of the Kinetic Constants. Comparison of Ignition Delays in Various Models. An analysis of the catastrophe/ignition manifold allows us to pass to a more concrete kinetic law of oxidation of a magnesium particle in air, taking into account c-phase evaporation. For this purpose, we write equations governing the preexplosion state [see (2)]:

$$\begin{aligned} ke^{-E'/T} - ve^{-E_1'/T} &= \alpha_0(T - \tilde{T}), \\ k\frac{E'}{T^2}e^{-E'/T} - v\frac{E_1'}{T^2}e^{-E_1'/T} &= \alpha_0, \end{aligned} \tag{6}$$

where $\alpha_0 = \lambda \mathrm{Nu}/2r_s\rho_s q$, the scale temperature is $T_s = 300$ K, and the activation energy E' and the heat of vaporization E_1' are referred to RT_s. According to the experimental data of Khaikin et al. [5], we assume $E_1' = 53.333$, and we calculate (6) at two arbitrary points $(r_{s,j}, \tilde{T}_j)_{j=1,2}$ of the experimental curve that describes the particle radius as a function of the limiting temperature of the ambient air [1, 2, 8]. This allows us to obtain a closed system of transcendental equations for determination of the unknown quantities E and k (if they exist) and the particle temperature at the ignition limit. Thus, we have found the kinetic parameters for $v = 0.15$ m/sec: $E' = 40.315$ ($E/R = 12{,}094$ K) and $k = 0.169$ m/sec for small particles (with radii of 15 to 60 μm) and $E' = 96.452$ ($E/R = 28{,}936$ K) and $k = 6.855 \cdot 10^5$ m/sec for large particles (with radii of 300 to 600 μm).

It is of interest to compare ignition delays resulting from these kinetic laws of oxidation with similar data of the evaporation-free model proposed in [1, 2]. As is seen from Table 4, the difference for small particles is insignificant. The difference for large particles is less than 11%.

CONCLUSION

A catastrophe/ignition manifold for a model of magnesium-particle ignition that takes into account the chemical oxidation reaction, metal evaporation, and convective heat exchange with the ambient gas has been analyzed qualitatively and quantitatively. This made it possible

- to locate the domains of ignition, extinction, and regular heating of the particle in the plane of governing parameters of the model;
- to find the kinetic constants in the empirical law of ignition;
- to show the stability of the integral parameter of the ignition delay in relation to sets of kinetic constants determined for mathematical models with and without account for metal evaporation.

REFERENCES

1. A. V. Fedorov, "Physicomathematical modeling of the ignition of small magnesium particles," Preprint No. 12-94, Inst. Theor. Appl. Mech., Sib. Div., Russian Acad. of Sciences, Novosibirsk (1994).
2. A. V. Fedorov, "Numerical and analytical study of magnesium-particle ignition," *Fiz. Goreniya Vzryva*, **32**, No. 1, 75–84 (1996).
3. Yu. A. Gosteev and A. V. Fedorov, "Magnesium-particle ignition (distributed model)," *Fiz. Goreniya Vzryva*, **32**, No. 4, 5–12 (1996).
4. M. B. Borovikov and U. I. Gol'dshleger, "Critical phenomena in a system with two parallel exothermic and endothermic reactions," *Dokl. Akad. Nauk SSSR*, **261**, No. 2, 392 (1981).
5. B. I. Khaikin, V. I. Bloshenko, and A. G. Merzhanov, "On ignition of metal particles," *Fiz. Goreniya Vzryva*, **6**, No. 4, 474–488 (1970).
6. E. V. Petukhova and A. V. Fedorov, "Ignition of magnesium particles near the end of a shock tube," *Fiz. Goreniya Vzryva*, **27**, No. 6, 139–142 (1991).
7. A. V. Fedorov and Yu. A. Gosteev, "Physical-mathematical investigation of magnesium particle ignition," in: Preprint of the 7th Int. Colloquium on Dust Explosions, Bergen, Norway (1996), pp. 2.58–2.74.
8. H. V. Cassel and I. Libman, "Combustion of magnesium particles. II. Ignition temperatures and thermal conductivities of ambient atmospheres," *Combust. Flame*, **7**, No. 1 (1963).